

Energy-Dependence of the Nucleon Self-Energies in Off-Mass-Shell Energy Region and the Gamow-Teller Sum-Rule in the Relativistic Hartree-Fock Approach

Tomoyuki Maruyama^{1,2}

¹*College of Bioresource Sciences, Nihon University, Fujisawa, Kanagawa 252-8510, Japan*

²*Advanced Science Research Center, Japan Atomic Energy Agency, Tokai, Ibaraki 319-11, Japan*

The relativistic Hartree approximation predicts a deep attractive potential for antinucleon, which largely reduce the threshold energies of the nucleon-antinucleon ($N\bar{N}$) production. This effect has played an important role to explain the quenching of the Gamow-Teller (GT) strength because the quenched strength in the particle-hole excitation is partially taken by the nucleon-antinucleon production. On the other hand antiproton experiments do not reveal deep attractive potential for antinucleon. In this paper we study energy-dependence of the nucleon self-energies in the relativistic Hartree-Fock (RHF) approximation in off-mass-shell states. Then we demonstrate that the antinucleon appearing in low energy observables is in the off-mass-shell energy region and that its properties are quite different from that at the on-mass-shell state. Furthermore we show that the quenched amount of the GT strength does not shift only to the $N\bar{N}$ production but also to the meson production through the imaginary part of the nucleon self-energy in the RHF approximation.

PACS numbers: 31.30.jg, 24.10.Jv

I. INTRODUCTION

The past decades have seen many successes in the relativistic mean-field (RMF) approach of the nuclear many-body problem. The relativistic framework has big advantages in several aspects [1]: a useful Dirac phenomenology for the description of nucleon-nucleus scattering [2, 3], the natural incorporation of the spin-orbit force [1] and the saturation properties in the microscopic treatment with the Dirac Brueckner Hartree-Fock (DBHF) approach [4]. Furthermore this approach can explain very nicely the structure of such extreme nuclei as for neutron-rich nuclei [5].

These results conclude that there are large attractive scalar and repulsive vector-fields, and that the nucleon effective mass becomes very small in the medium. These deep scalar and vector fields predict very strong attractive potential of antinucleon (\bar{N}) and large suppression of the in-medium threshold energy of the nucleon-antinucleon ($N\bar{N}$) pair creation because the vector fields is changed to be attractive for \bar{N} .

Kurasawa and Suzuki [6, 7] showed that the largely reduced threshold energy of $N\bar{N}$ production in medium play a very important role to explain the suppression of the Coulomb sum-rule in the quasielastic electron scattering. Furthermore they showed that the Gamow-Teller (GT) transition strength is quenched by the antinucleon degree of freedom [8, 9]. The particle-hole (ph) excitation explains 88 % of the Ikeda-Fujii-Fujita (IFF) sum-rule, and the other 12 % strength is given by the $N\bar{N}$ -production. The shift of the strength from the ph -excitation sector to the $N\bar{N}$ -production sector increases as the effective mass becomes smaller [10].

In the RMF approach, thus, the largely reduced threshold energy play important roles in calculations of several low energy phenomena. However experimental observables about the antiproton have not revealed this deep \bar{N} attractive potential. For example the analysis of the antiproton (\bar{p}) + nucleus elastic scattering has not shown its deep attractive potential [11]. Furthermore Teis et al. [12] analyzed the subthreshold \bar{p} -production experiments in nucleus-nucleus collisions [13] and light-ion induced collisions [14] and concluded that the \bar{p} mean-field is attractive but its depth is much smaller than that predicted in the RH approximation. Particularly the results in the light-ion induces reactions gave important results that the the cross-section in the deuteron induced reaction, σ_d , is fifty times larger than that in the proton induced reaction, σ_p at the initial energy, $E_{lab} = 3.5$ GeV/u: $\sigma_d/\sigma_p \approx 50$. If the \bar{p} potential is as deep as that in the RH approximation, this initial energy is above the threshold energy, and the ratio must be close to the nucleon number of the induced particles, namely $\sigma_d/\sigma_p \approx 2$.

Of course there are some ambiguities even in theoretical analysis of experimental results. For example, G.Q. Li et al. [15] gave a different conclusion about the analysis of the GSI experiments [13] though they have not shown any analysis about the KEK data [14]. We cannot definitely determine the \bar{N} potential, but these experimental results suggests suspicion on the treatment of the antinucleon in the RMF approach.

In the theoretical aspect only the RH approximation suggests the deep \bar{N} potential, but one can deny it by extending the theory, such as the relativistic Hartree-Fock (RHF), including the nonlocal parts [16]. In the RHF framework, furthermore, the self-energies of nucleon are momentum-dependent and have different values between the on-mass-shell state and the off-mass-shell states [17]. The antinucleon

appearing in calculations of low energy phenomena must be at an off-mass-shell state, and its property may be different from that at the on-mass-shell state. If the antinucleon properties at the off-mass-shell state is different, moreover, we need to examine the transition strength in the $N\bar{N}$ -production.

In this subject, it has been believed for a long time that the momentum-dependence of the Dirac fields is negligible in the low energy region, particularly below the Fermi level. In fact, only very small momentum-dependence has appeared in the RHF calculation [18]. In the high energy region, however, the vector-fields must become very small to explain the optical potential of the proton-nucleus elastic scattering [2, 17], and the transverse flow in the heavy-ion collisions [19]. In addition this momentum-dependence also play an important role to explain the quasielastic electron scattering [20]. Even in low energy region, furthermore, the momentum dependence has been reported to plays important roles to explain the isoscalar giant quadrupole resonance [21], the spatial convection current [22], nuclear structure [23] and the pseudo-spin symmetry [24]. In addition the DBHF approach also slightly change a saturation properties if the momentum dependence is introduced [25].

In this paper we examine the energy-dependence of the Dirac mean-field in the RHF approximation and show the antinucleon properties in off-mass-shell energy region. Furthermore we calculate the GT-strength in the same approach.

In Sec. II we explain structures of the nucleon propagator and self-energies in the RHF approach. In Sec. III we calculate the energy-dependence of the nucleon self-energies and demonstrate that the $N\bar{N}$ -production energy appearing in calculations is energy-dependent and different from that in the actual production. In Sec. IV we calculate the GT strength and demonstrate that this strength is contributed from three processes, the ph -excitation, the $N\bar{N}$ -production and the meson production. Finally we summarize our work in Sec. V.

II. NUCLEON PROPAGATOR WITH MOMENTUM-DEPENDENT SELF-ENERGIES

The nucleon propagator in the self-energy Σ is usually given by

$$G^{-1}(p) = \not{p} - M - \Sigma(p), \quad (1)$$

where $\Sigma(p)$ has a Lorentz scalar part U_s and a Lorentz vector part $U_\mu(p)$ as

$$\Sigma(p) = -U_s(p) + \gamma^\mu U_\mu(p). \quad (2)$$

For the future convenience we define the effective mass and the kinetic momentum as

$$\begin{aligned} M^*(p) &= M - U_s(p), \\ \Pi_\mu(p) &= p_\mu - U_\mu(p). \end{aligned} \quad (3)$$

Then the detailed form of the nucleon propagator, $G(p)$, is represented [17] by

$$\begin{aligned} G(p) &= G_F(p) + G_D(p) \\ &= \frac{\gamma^\mu \Pi_\mu(p) + M^*(p)}{\Pi^2(p) - M^{*2}(p) + i\delta} + i\pi n(\mathbf{p})\theta(p_0) [\gamma^\mu \Pi_\mu(p) + M^*(p)] \delta[V(p)], \end{aligned} \quad (4)$$

where $n(\mathbf{p}) = \theta(k_F - |\mathbf{p}|)$ is the momentum distribution with the Fermi momentum, k_F , and

$$V(p) \equiv \frac{1}{2} [\Pi^2(p) - M^{*2}(p)]. \quad (5)$$

Now we will rewrite the above nucleon propagator in the spectral representation. The wave-function of nucleon, $\psi(p, s)$, with four-momentum p and spin s is defined as a solution of the following Dirac equation

$$[\gamma^\mu \Pi_\mu(p) - M^*(p)] \psi(p, s) = 0. \quad (6)$$

This Dirac equation is equivalent to the following characteristic equation:

$$[\vec{\alpha} \cdot \vec{\Pi}(p_0; \mathbf{p}) - \beta M^*(p_0; \mathbf{p}) + U_0(p_0; \mathbf{p})] \psi(p, s) = \lambda \psi(p, s). \quad (7)$$

There are two kinds of solutions; one is so-called a positive energy spinor $u(p, s)$ with

$$\lambda = e_N(p) \equiv E_N(p) + U_0(p) = \sqrt{\Pi_v^2(p) + M^{*2}(p)} + U_0(p), \quad (8)$$

and the other is called a negative energy spinor $v(-p, s)$ with

$$\lambda = -e_A(p) \equiv -E_N(p) + U_0(p) = -\sqrt{\Pi_v^2(p) + M^{*2}(p)} + U_0(p), \quad (9)$$

where s is a spin-index, and $\Pi_v(p) \equiv |\vec{\Pi}(p)| = \hat{p} \cdot \vec{\Pi}(p)$. Note that e_N and e_A are dependent on four momentum p and are not the single particle energies at the on-mass-shell states.

Using the above spinors and energies, we can get the following relations:

$$(p_0 - e_N(p))(p_0 + e_A(p)) = \Pi^2(p) - M^{*2}(p), \quad (10)$$

$$\sum_s u(p, s) \bar{u}(p, s) \equiv \Lambda_+(p) = \frac{E_N(p) \gamma_0 - \vec{\Pi}(p) \cdot \vec{\gamma} - M^*(p)}{2E_N(p)}, \quad (11)$$

$$\sum_s v(-p, s) \bar{v}(-p, s) \equiv \Lambda_-(p) = \frac{E_N(p) \gamma_0 + \vec{\Pi}(p) \cdot \vec{\gamma} + M^*(p)}{2E_N(p)}. \quad (12)$$

Then, the nucleon propagator (4) can be rewritten as

$$\begin{aligned} G(p) = & \sum_s (1 - n(\mathbf{p})) \frac{u(p, s) \bar{u}(p, s)}{p_0 - e_N(p) + i\delta} + \sum_s n(\mathbf{p}) \frac{u(p, s) \bar{u}(p, s)}{p_0 - e_N(p) - i\delta} \\ & + \sum_s \frac{v(-p, s) \bar{v}(-p, s)}{p_0 + e_A(p) - i\delta}. \end{aligned} \quad (13)$$

This expression is the same as the single nucleon propagator which was given by Bentz et al. as the general form [28]. The first, second and third terms exhibit contributions from nucleons above the Fermi surface, nucleon in the Fermi sea and negative energy nucleons in the Dirac sea, respectively. Furthermore, the on-mass-shell positive energy, ε_N , and the negative energy, ε_A , are defined as the pole energies of the propagator in Eq.(13):

$$\varepsilon_N(\mathbf{p}) = e_N(p_0 = \varepsilon_N; \mathbf{p}), \quad (14)$$

$$\varepsilon_A(\mathbf{p}) = e_A(p_0 = -\varepsilon_A; \mathbf{p}). \quad (15)$$

We should here note the orthogonal relations between the Dirac spinors. The Dirac spinors of the positive energy state, $u(p, s)$, and negative energy state, $v(-p, s)$, are orthogonal only at the same energy, p_o :

$$v^\dagger(-p_0; -\mathbf{p}, s) u(p_0; \mathbf{p}, s') = 0. \quad (16)$$

but the two spinors on the on-mass-shell condition are not orthogonal

$$v^\dagger(\varepsilon_A(\mathbf{p}); -\mathbf{p}, s)u(\varepsilon_N(\mathbf{p}); \mathbf{p}, s') \neq 0. \quad (17)$$

The positive energy projection operator, $\Lambda_+(p)$, and the negative energy projection operator, $\Lambda_-(p)$, with the same p_0 satisfy the usual relation,

$$\{\Lambda_+(p_0; \mathbf{p}) + \Lambda_-(p_0; \mathbf{p})\} \gamma_0 = 1, \quad (18)$$

but those with the on-mass-shell energy do not satisfy this relation:

$$\{\Lambda_+(\varepsilon_N(\mathbf{p}); \mathbf{p}) + \Lambda_-(-\varepsilon_A(\mathbf{p}); \mathbf{p})\} \gamma_0 \neq 1. \quad (19)$$

This fact tells us a problem in the sum rule. For an example, the energy non-weighted sum-rule with respect to a single particle transition operator, \mathcal{O} , can be obtained with the single particle wave functions as

$$S = \sum_s \int \frac{d^3p}{(2\pi)^3} n(\mathbf{p}) u^\dagger(\mathbf{p}, s) \mathcal{O}^\dagger \mathcal{O} u(\mathbf{p}, s) \quad (20)$$

$$= \sum_s \int \frac{d^3p}{(2\pi)^3} n(\mathbf{p}) u^\dagger(\mathbf{p}, s) \mathcal{O}^\dagger \Lambda_+ \mathcal{O} u(\mathbf{p}, s) + \sum_s \int \frac{d^3p}{(2\pi)^3} n(\mathbf{p}) u^\dagger(\mathbf{p}, s) \mathcal{O}^\dagger \Lambda_- \mathcal{O} u(\mathbf{p}, s). \quad (21)$$

In the RH approximation the first and second terms show the contributions from the ph -states and the $N\bar{N}$ -states, respectively. In the RHF approximation, however, the first term also shows the ph -contribution but the second term dose not completely correspond to the $N\bar{N}$ -contribution.

III. SELF-ENERGIES IN THE RELATIVISTIC HARTREE-FOCK APPROXIMATION

In this section we should give the detailed expressions of the momentum-dependent self-energies. In order to discuss these effects up to the $N\bar{N}$ -threshold energies, we need to take into account many kinds of diagrams with multi-meson exchanges. In this work, however, we aim to demonstrate only qualitative effects of the momentum dependence, and then we use the RHF approximation within the one-meson exchanges. Furthermore we omit the isovector parts of the self-energies. In this work we discuss only qualitative effects of their momentum dependence in the system with very small asymmetry between the proton and neutron numbers.

The nucleon self-energy is separated into the Hartree part and the Fock part as

$$\Sigma(p) = \Sigma_H + \Sigma_F(p) = -(U_s^H + U_s^F(p)) + \gamma^\mu (U_\mu^H + U_\mu^F(p)), \quad (22)$$

where $\alpha = s, \mu$. Within the one-boson exchange force, the Fock part of the self-energy is generally written in the following way [17, 18, 19].

$$\begin{aligned} \Sigma_F(p) = & i \sum_a f_a g_a^2 \int \frac{d^4k}{(2\pi)^4} \gamma^a G(k) \gamma_a \Delta_a(p-k) \\ & + i \sum_b \tilde{f}_b \tilde{g}_b^2 \int \frac{d^4k}{(2\pi)^4} [(\not{p} - \not{k}), \gamma^b] G(k) [\gamma_b, (\not{p} - \not{k})] \Delta_b(p-k), \end{aligned} \quad (23)$$

where $\gamma_{a(b)}$ is the γ -matrix with the suffix $a(b)$ indicating the scalar, pseudo-scalar, vector, axial-vector and tensor, and Δ_a is the propagator of meson with the quantum number indicated with the suffix a , written as

$$\Delta_a(q) = \frac{1}{m_a^2 - q^2 - i\delta}. \quad (24)$$

In addition $g_a(\tilde{g}_b)$ is a coupling constant, and $f_a(\tilde{f}_b)$ is a certain factor including the Fiertz transformation coefficient in the isospin space and so on.

In general the Fock part of the nucleon self-energy is written as

$$U_s^F(p) = \sum_a C_a^{(s)} \int \frac{d^3\mathbf{k}}{(2\pi)^3} n(\mathbf{k}) \frac{M^*(k)}{\tilde{\Pi}_0(k)} \Delta_a(p-k), \quad (25)$$

$$U_\mu^F(p) = U_\mu^{(1)}(p) + U_\mu^{(2)}(p) \quad (26)$$

with

$$U_\mu^{(1)}(p) = \sum_a C_a^{(v)} \int \frac{d^3\mathbf{k}}{(2\pi)^3} n(\mathbf{k}) \frac{\Pi_\mu(k)}{\tilde{\Pi}_0(k)} \Delta_a(p-k), \quad (27)$$

$$U_\mu^{(2)}(p) = \sum_b \tilde{C}_b^{(v)} \int \frac{d^3\mathbf{k}}{(2\pi)^3} n(\mathbf{k}) \frac{\Pi(k) \cdot (p-k)}{\tilde{\Pi}_0(k)} (p_\mu - k_\mu) \Delta_b(p-k), \quad (28)$$

where

$$\tilde{\Pi}_\mu(p) = \frac{\partial V(p)}{\partial p^\mu}. \quad (29)$$

Note that some meson exchanges such as the pseudo-scalar meson with the PV coupling give a different expression which is proportional to $(p-k)^2 \Delta(p-k)$. However these terms can be rewritten to the same expression of the above equation by introducing the cut-off parameters whose contribution can be incorporated into the Hartree parts [21, 22].

According to the way in Ref.[17, 19, 21, 22], we give the Hartree part of the self-energies are given as

$$U_s^H = g_s^H \phi \quad (30)$$

$$U_\mu^H = \delta_\mu^0 \left(\frac{g_v^H}{m_v} \right)^2 \rho_H \quad (31)$$

where ϕ is the scalar mean-field obtained as

$$\frac{\partial}{\partial \phi} \tilde{U}[\phi] = g_s^H \rho_s \quad (32)$$

In the above equations the scalar density ρ_s and the vector Hartree density ρ_H are given by

$$\rho_s = 4 \int \frac{d^3\mathbf{p}}{(2\pi)^3} n(\mathbf{p}) \frac{M_\alpha^*(p)}{\tilde{\Pi}_0(p)}, \quad (33)$$

$$\rho_H = 4 \int \frac{d^3\mathbf{p}}{(2\pi)^3} n(\mathbf{p}) \frac{\Pi_0(p)}{\tilde{\Pi}_0(p)}. \quad (34)$$

The self-energy potential of the ϕ -field is given [19, 21, 22] by

$$\tilde{U}[\phi] = \frac{\frac{1}{2}m_s^2\phi^2 + \frac{1}{3}B_s\phi^3 + \frac{1}{4}C_s\phi^4}{1 + \frac{1}{2}A_s\phi^2}. \quad (35)$$

Here we comment a relation between the RH and RHF approximations. In the RMF approach one usually determines the meson-nucleon coupling constants to reproduce the saturation properties of the nuclear matter. When $m_a \gg k_F$, the zero range approximation is available, and the above Fock terms (25) and (27) approximately become

$$U_s^F(p) = \sum_a \frac{C_a^{(s)}}{m_a^2} \int \frac{d^3\mathbf{k}}{(2\pi)^3} n(\mathbf{k}) \frac{M^*}{E_k^*} = \left(\sum_a \frac{C_a^{(s)}}{4m_a^2} \right) \rho_s, \quad (36)$$

$$U_\mu^F(p) = \sum_a \frac{C_a^{(v)}}{m_a^2} \int \frac{d^3\mathbf{k}}{(2\pi)^3} n(\mathbf{k}) \frac{k^*}{E_k^*} = \delta_\mu^0 \left(\sum_a \frac{C_a^{(v)}}{4m_a^2} \right) \rho_B. \quad (37)$$

These terms are equivalent to the Hartree parts of the self-energies. Under this approximation, thus, the Hartree and Fock contributions cannot be distinguished, and parameterizing the Hartree parts independently from the Fock parts is the same as introducing heavy mesons in the RHF calculation. Therefore we do not need to take the scalar and vector coupling constants, g_s^H and g_v^H , to be the same ones in the Fock parts. Indeed Weber et al. [17] have shown that this method does not break significant conservation laws as for the nuclear current and the energy-momentum tensor.

In this work we discuss the self-energies at off-shell energy states, where their imaginary parts appear in some energy region [17]. In the actual calculation it is not very easy to calculate the Fock parts when the imaginary parts appear, and then we introduce an additional approximation as follows.

Below the Fermi level with the on-mass-shell condition, the momentum dependence of the self-energies is not large [18] and can be neglected in actual calculations. Then we make the self-energies in the integrands in Eqs.(25), (27) and (28) momentum-independent by fixing their values to be those at the Fermi momentum on the on-mass-shell condition: $U_{s(0)} = U_{s(0)}(\varepsilon_F; k_F)$ and $U_i = 0$, where ε_F is the Fermi energy; the similar method was used in the DBHF calculation [4]. When the self-energies are momentum-independent, the tensor-coupling part of the vector self-energy (28) is very small and can be disregarded [18]. Then the momentum-dependent parts of the self-energies approximately become

$$U_s^F(p) = \int \frac{d^3\mathbf{k}}{(2\pi)^3} n(\mathbf{k}) \frac{M^*}{E_k^*} \sum_a \frac{C_a^{(s)}}{m_a^2 - (E_k^* + U_0(k_F) - p_0)^2 + (\mathbf{k} - \mathbf{p})^2 - i\delta}, \quad (38)$$

$$U_\mu^F(p) = \int \frac{d^3\mathbf{k}}{(2\pi)^3} n(\mathbf{k}) \frac{k^*}{E_k^*} \sum_a \frac{C_a^{(v)}}{m_a^2 - (E_k^* + U_0(k_F) - p_0)^2 + (\mathbf{k} - \mathbf{p})^2 - i\delta}, \quad (39)$$

where $E_k^* = \sqrt{k^2 + M^{*2}(k_F)}$ and $k^* = (E_k^*, \mathbf{k})$.

In the actual numerical calculations we consider the Hartree-parts, U_s^H and U_0^H , as fitting parameters, and determine their values to reproduce the saturation properties, $BE = M - \varepsilon_N(k_F)$ and $M^*(k_F)$, at the saturation density.

Now we perform the RHF calculation and discuss effects of the momentum dependence in the self-energies in the off-shell energy region.

When π (PV), η (PV), σ , δ , ω meson exchanges are introduced, the Fock terms are described with the following meson propagations:

$$\sum_a C_a^{(s)} \Delta_a(q) = -\frac{3}{2} f_\pi^2 \Delta_\pi - \frac{1}{2} f_\eta^2 \Delta_\eta - \frac{1}{2} g_\sigma^2 \Delta_\sigma - \frac{3}{2} g_\delta^2 \Delta_\delta + 2g_\omega^2 \Delta_\omega + \frac{12g_\rho^2 - 9f_\rho^2}{2} \Delta_\rho \quad (40)$$

$$\sum_a C_a^{(v)} \Delta_a(q) = \frac{3}{2} f_\pi^2 \Delta_\pi + \frac{1}{2} f_\eta^2 \Delta_\eta + \frac{1}{2} g_\sigma^2 \Delta_\sigma + \frac{3}{2} g_\delta^2 \Delta_\delta + g_\omega^2 \Delta_\omega + \frac{6g_\rho^2 + 3f_\rho^2}{2} \Delta_\rho, \quad (41)$$

where f_ρ is the tensor coupling of the ρ -N interaction. In this work we use the two parameter-sets in the actual numerical calculations.

The first set is so called the parameter HF(c), which is given in Ref.[18], $g_s^H = g_\sigma = 9.116$, $g_v^H = g_\omega = 10.39$, $m_\sigma = 550$ MeV, $m_\omega = 780$ MeV and the other couplings being zero.

This HF(C) parameter-set is standard in the RHF calculation, but it includes only the σ and ω mesons. In the next section, however, we discuss effects of the Fock terms in the IFF sum-rule, where all the kinds of mesons contribute to the result. Though we do not aim to get any qualitative conclusion in this work, therefore, we should use the mass and the couplings of mesons determined experimentally if possible. As the second parameter-set, then, we use the couplings and the meson masses in the Bonn-A potential [26] for the Fock parts. We determine the parameters in the Hartree parts as $g_s^H = 10.58$, $g_v^H = 5.338$, $B_s = 26.19\text{fm}^{-1}$, $C_s = 0$ and $A_s = 5.174\text{fm}^2$ with $m_s = 550\text{MeV}$ and $m_v = 780\text{MeV}$. to reproduce the saturation properties of the nuclear matter as the binding energy, $BE = 16$ MeV, the incompressibility, $K = 250\text{MeV}$, and the effective mass, $M^* = 0.6M$, at the Fermi momentum, $k_F = 1.36\text{fm}^{-1}$.

We show the momentum dependence of the scalar self-energy $U_s(p)$ and that of the time component of the vector self-energy $U_0(p)$ on the on-mass-shell condition with HF(c) in Fig. 1a and with Bonn-A in Fig. 1b. The solid and dashed represent the results of our approach, and the solid circles indicate the results in the fully self-consistent RHF calculations with Eqs.(25) and (27). For comparison, we plot $U_s(k_F)$ and $U_0(k_F)$ with the dashed lines; we refer to the calculation without the momentum-dependence of the self-energies as the RH calculation. In the two parameter-sets, our approximate approach for the Fock terms in (38) and (39) gives the same results of the full RHF calculations.

Next we discuss the energy dependence of the self-energies at the fixed momentum. In Fig. 2 we show the scalar self-energies, $U_s(p_0, k_F)$ and a time-component of the vector self-energies, $U_0(p_0, k_F)$ with HF(C) as functions of the nucleon energy, p_0 . Furthermore, $U_s(p_0, k_F)$ and $U_0(p_0, k_F)$ with Bonn-A are shown in Fig. 3. Their real parts and imaginary parts are plotted in the upper and lower panels, respectively. In the both results with different parameters the real parts of the self-energies have large energy dependence, particularly in the energy region, $0.5\text{GeV} \gtrsim p_0 - M \gtrsim 1.2\text{GeV}$, where the imaginary parts have large values. In addition the self-energies around the negative energy on-mass shell energy, $p_0 - M \approx (-1300) - (-1800)$ MeV, shows the different values from those around the on-mass-shell positive energy, $p_0 - M \approx -16$ MeV.

When we calculate observables in low energy phenomena, on the other hand, the negative energy states, which appear as the intermediate states, are in the off-mass-shell energy region. As an example we consider the situation that off-mass-shell meson with energy q_0 changes to nucleon and antinucleon, which often appears in one-loop calculation. When we assume that energy of the nucleon is the Fermi energy ε_F , the energy of the antinucleon is at the energy state $p_0 = q_0 - \varepsilon_F$, and its self-energies are those on $\varepsilon_F = q_0$. In studies about low energy phenomena $|q_0| \ll 0$, the self-energies are considered to be at $p_0 \approx \varepsilon_F$, and they do not have so large momentum-dependence around the Fermi surface. When we calculate such low energy phenomena, hence, we must use the same self-energies of the nucleon even for the negative energy nucleon.

Here we give an example. The energy denominator of the $N\bar{N}$ -contribution part in correlation functions is written as

$$D_{N\bar{N}}(p, q) = e_N(p) + e_A(p - q) - q_0. \quad (42)$$

When $D_{N\bar{N}} \ll 2M - q_0$, one considers that the $N\bar{N}$ -production process in the intermediate state make large contributions to calculational results.

Here we compare $D_{N\bar{N}}(q_0)$ in the RHF and RH approximations where the self-energies are momentum-independent. In order to make discussion easy, we calculate them with $\mathbf{q} = 0$, $|\mathbf{p}| = k_F$ and $p_0 = e_N = \varepsilon_F$, where the above energy denominator becomes

$$D_{N\bar{N}}(\varepsilon_F; k_F, q_0; 0) \equiv d_{N\bar{N}}(q_0) = \varepsilon_F + e_A(\varepsilon_F - q_0, k_F) - q_0. \quad (43)$$

We show $d_{N\bar{N}}(q_0)$ as a function of the energy transfer, q_0 , with HF(C) in Fig. 4 and those with Bonn-A in Fig. 5. The solid and dashed lines represent the results in the RHF and RH approximations, respectively. For comparison we plot the results in the vacuum, $M^* = M$, with the long-dashed line.

In the RH approximation $d_{N\bar{N}}$ has only a real part which is a linear function of q_0 and no imaginary part, while that in the RHF approximation exhibits a different behavior. As q_0 increases, the real part $\text{Re}d_{N\bar{N}}$ is almost the same as that in the RH approximation below $q_0 \approx 0.5$ (GeV), but shows a quite complicated behavior in $q_0 \gtrsim m_\sigma = 0.55$ GeV, where the imaginary part becomes large; the qualitative behaviors are almost same when the parameters are HF(C) and Bonn-A.

Furthermore, the $N\bar{N}$ -production threshold energy, where $d_{N\bar{N}}(q_0) = 0$, is about $q_0 \approx 1250$ MeV in the RH calculation and $q_0 \approx 1630$ MeV in the RHF calculation. The threshold energy in the RHF approximation is still smaller than that in the vacuum, $2M \approx 1880$ MeV, but less drastic than that in the RH approximation.

When $q_0 \lesssim 300$ MeV, the amount of $d_{N\bar{N}}$ in the RHF approximation is almost the same as that in the RH approximation, and much smaller than that in the vacuum. In both the RHF and RH approximations the threshold energy of the $N\bar{N}$ -production is seen to be largely reduced from that in the vacuum when the energy transfer is very low and far from the on-mass-shell condition.

In high energy transfer region, $q_0 \gtrsim 500$ MeV, however, the RH and RHF calculations give quite different results. The actual threshold energy of the $N\bar{N}$ -production energy is also different between two approaches. Even if the suppressed threshold energy is estimated from low energy phenomena in the RMF approach, we cannot conclude that the estimated amount of the threshold energy is the same as that in the actual $N\bar{N}$ -production.

IV. GAMOW-TELLER STRENGTH

Because of the energy dependence of the nucleon self-energies, the correlation function must show quite different behaviors in the energy region above about 300 MeV between the RH and RHF approximations. Indeed, Weber et al. [17] suggested that the imaginary part of the self-energies make another contribution to the nucleon spectral function besides the nucleon states on the on-mass-shell positive and negative energy states.

In this section we examine contributions from the Fock terms of the self-energies to the GT strength. Here we calculate the GT strength in the impulse approximation. The random phase approximation (RPA) has not given so different amount of the GT strength from that in the impulse approximation [8]. Here we define the GT-correlation functions as

$$C_{GT}(q) = C_{\beta-}(q) - C_{\beta+}(q) \quad (44)$$

with

$$C_{\beta-}(q) \equiv C_A(q) = -i \int \frac{d^4 p}{(2\pi)^4} \text{Tr} \{ G(p+q) \gamma_5 \gamma_2 \tau_- G(p) \gamma_5 \gamma_2 \tau_+ \} \quad (45)$$

$$\begin{aligned} C_{\beta+}(q) &= -i \int \frac{d^4 p}{(2\pi)^4} \text{Tr} \{ G(p+q) \gamma_5 \gamma_2 \tau_+ G(p) \gamma_5 \gamma_2 \tau_- \} \\ &= -i \int \frac{d^4 p}{(2\pi)^4} \text{Tr} \{ G(p-q) \gamma_5 \gamma_2 \tau_- G(p) \gamma_5 \gamma_2 \tau_+ \} = C_A(-q). \end{aligned} \quad (46)$$

By substituting Eq.(4) into Eq.(44) and disregarding the vacuum polarization and the isovector part of the self-energies, we can obtain the correlation function as

$$\begin{aligned} C_{GT}(q) &= \frac{4}{(2\pi)^3} \int \frac{d^3 p}{\tilde{\Pi}_0(p)} \left[n^{(n)}(\mathbf{p}) - n^{(p)}(\mathbf{p}) \right] \\ &\times \left[\frac{t_A(p, q)}{\Pi^2(p+q) - M^{*2}(p+q) + i\delta} - \frac{t_A(p, -q)}{\Pi^2(p-q) - M^{*2}(p-q) + i\delta} \right] \end{aligned} \quad (47)$$

with

$$t_A(p, q) = \Pi_0(p+q) \cdot \Pi_0(p) - \frac{1}{3} \Pi_v(p+q) \Pi_v(p) + M^*(p+q) M^*(p) \quad (48)$$

where $\Pi_v(p) = \mathbf{p} \cdot \Pi$. In addition $n^{(n)}(\mathbf{p}) = \Theta(k_n - |\mathbf{p}|)$ and $n^{(p)}(\mathbf{p}) = \Theta(k_p - |\mathbf{p}|)$ are the momentum distributions for neutron and proton, where k_n and k_p being the neutron and proton Fermi momenta, respectively.

In the GT-transition we consider only the zero momentum transfer, $\mathbf{q} = 0$, and the positive energy transfer, $q_0 > 0$. When $|\rho_n - \rho_p| \ll \rho_B$, in addition, we can use the following relation

$$n^{(n)}(\mathbf{p}) - n^{(p)}(\mathbf{p}) \approx \frac{\pi^2}{2k_F^2} a_r \delta(|\mathbf{p}| - k_F) \quad (49)$$

with

$$a_r = \frac{2(N-Z)}{A} \rho_B, \quad (50)$$

where ρ_B is the baryon density. Then the correlation function at $\mathbf{q} = 0$ becomes

$$\begin{aligned} &C_{GT}(q_0; \mathbf{q} = 0) \\ &= \frac{a_r}{2\tilde{\Pi}_0(k_F)} \left\{ \frac{t_A(p, q)}{E_N(p+q) [q_0 + \varepsilon_F - e_N(p) + i\delta]} \right. \\ &\quad - \frac{t_A(p, q)}{E_N(p+q) [q_0 + \varepsilon_F + e_A(p+q) + i\delta]} \\ &\quad - \frac{t_A(p, -q)}{E_N(p-q) [q_0 + \varepsilon_F - e_N(p-q) - i\delta]} \\ &\quad \left. + \frac{t_A(p, -q)}{E_N(p-q) [q_0 + \varepsilon_F + e_A(p-q) - i\delta]} \right\}_{p=(\varepsilon_F; k_F), q=(q_0; 0)}. \end{aligned} \quad (51)$$

The response function is defined as

$$R_{GT}(q_0) = -\frac{1}{\pi} \text{Im} C_{GT}(q_0; \mathbf{q} = 0) = a_r [R_{ph}(q_0) + R_{N\bar{N}}(q_0) + R_m(q_0)] \quad (52)$$

with

$$R_{ph} = \frac{\Pi_0^2(k_F) - \frac{2}{3}\Pi_v^2(k_F)}{\tilde{\Pi}_0^2(k_F)} \delta(q_0) \quad (53)$$

$$R_{N\bar{N}} = \frac{2\Pi_v^{*2}}{3\tilde{\Pi}_0(k_F)\tilde{\Pi}_0(-\varepsilon_A(k_F); k_F)} \delta(q_0 - \varepsilon_F - \varepsilon_A(k_F)). \quad (54)$$

In the above equations R_{ph} and $R_{N\bar{N}}$ show the contributions from the ph -excitation and the $N\bar{N}$ -production, respectively. The other term, R_m , indicates the contribution from the meson production, which comes from the imaginary parts of the self-energies.

Using Eq.(52) the total GT strength is obtained as

$$\begin{aligned} S_{tot} &= \Omega \int_0^\infty dq_0 R_{GT}(q_0) = S_{ph} + S_{N\bar{N}} + S_{meson} \\ &= 2(N - Z) \left(\tilde{S}_{ph} + \tilde{S}_{N\bar{N}} + \tilde{S}_{meson} \right) \end{aligned} \quad (55)$$

with

$$\tilde{S}_{ph} = \frac{\Pi_0^2(k_F) - \frac{2}{3}\Pi_v^2(k_F)}{\tilde{\Pi}_0^2(k_F)}, \quad (56)$$

$$\tilde{S}_{N\bar{N}} = \frac{2\Pi_v^{*2}}{3\tilde{\Pi}_0(k_F)\tilde{\Pi}_0(-\varepsilon_A(k_F); k_F)}, \quad (57)$$

$$\tilde{S}_{meson} = \int_0^\infty dq_0 R_m(q_0), \quad (58)$$

where Ω is the volume of the system.

In the RH approximation the relativistic self-energies are momentum-independent, and the above response function has been given in Ref. [8] as

$$\tilde{S}_{ph} = 1 - \frac{2}{3} \frac{k_F^2}{E_F^{*2}}, \quad (59)$$

$$\tilde{S}_{N\bar{N}} = \frac{2}{3} \frac{k_F^2}{E_F^{*2}}, \quad (60)$$

where the meson production part does not appear, $\tilde{S}_{meson} = 0$. The ph -contribution of the GT-strength is seen to be quenched, though the sum of the two strengths satisfies the IFF sum-rule [8] as

$$S_{ph} + S_{N\bar{N}} = S_{IFF} \equiv 2(N - Z). \quad (61)$$

In the RHF framework, on the other hand, the kinetic momentum Π_μ has energy dependence even if the spacial component of the momentum is fixed; namely $\Pi_{0(v)}(\varepsilon_F; k_F) \neq \Pi_{0(v)}(-\varepsilon_A(k_F); k_F)$.

When we use the HF(C) parameters, $S_{ph}/S_{IFF} \approx 0.84$ and $S_{ph}/S_{IFF} \approx 0.27$ in the present RHF calculation while $S_{ph}/S_{IFF} \approx 0.84$ and $S_{ph}/S_{IFF} \approx 0.16$ in the RH calculation. When we use the Bonn-A parameters, $S_{ph}/S_{IFF} \approx 0.88$ and $S_{ph}/S_{IFF} \approx 0.249$ in the present RHF calculation while $S_{ph}/S_{IFF} \approx 0.87$ and $S_{ph}/S_{IFF} \approx 0.13$ in the RH calculation: $(S_{ph} + S_{N\bar{N}})/S_{IFF} \approx 0.11$ in the RHF calculation with the above two parameter-sets.

As shown before, there is the meson production part of the response function, $2a_\tau R_m(q_0)$, in the RHF approximation, which also contributes to the sum-rule. In Fig. 6 we show the calculational results of $R_m(q_0)$ in the RHF approximation with HF(C) (a) and Bonn-A (b).

In this paper we do not intend to discuss the quenching of the GT-strength, and then we do not introduce several important effects such as the chains of the ring diagrams [9, 10] appearing in RPA, diagram of the direct meson production process, the delta excitation of nucleon [27, 29] and the two-particle two-hole excitation [30].

Thus our results do not give any qualitative conclusions, but it can successfully demonstrate that the suppression of the strength in the ph -sector does not shift only to the $N\bar{N}$ -production but also to the meson production sector in the relativistic framework.

V. SUMMARY

In this paper we calculate the nucleon self-energies and show their energy dependence in off-mass-shell energy region in the RHF approximation. We use the two parameter-sets and confirm that the calculations with the different parameters give qualitatively similar results.

The single particle energies of nucleon and antinucleon appearing in the denominator part of the nucleon propagator also have energy dependence. This energy dependence can simultaneously explain the two apparent inconsistent results, the analysis about the Coulomb sum-rule [6, 7] and the GT sum-rule [8, 9] and the analysis of the \bar{p} -production experiments [12]. The former study suggested the large suppression of the $N\bar{N}$ -production energy, and the latter one denied it. Our result demonstrates that the estimation of the $N\bar{N}$ -production energy depends on the energy region. When we study low energy phenomena, the energy of $N\bar{N}$ -production in the RHF approximation is seen to be almost the same as that in the RH approximation and much smaller than that in the vacuum. In the $N\bar{N}$ -production, however, the production energy becomes larger in the RHF approximation than that in the RH approximation.

Furthermore, we calculate the response function of the GT transition. In the meson production energy region the nucleon self-energies have imaginary parts and contribute to the GT response function. Then the quenched strength of the GT transition in the ph -excitation sector does not shift only to the $N\bar{N}$ -production sector but also to the meson production sector in the relativistic framework.

For simplicity we consider only contribution from the nucleon self-energies in the present calculations. In order to get quantitative conclusions, we need to introduce some other effects such as the RPA contributions and the multi-particle multi-hole excitations and so on.

Furthermore, the RHF calculation with the one-boson-exchange does not give the imaginary part of the antinucleon self-energies. The antinucleon in medium are largely absorbed by colliding with nucleons, and its self-energies must have large imaginary part. The two contributions from the meson and $N\bar{N}$ productions cannot be either distinguished in actual experiments and more realistic calculations beyond the Hartree-Fock approximation including multi-boson exchanges.

Anyway the RMF approach based on the RH approximation must be useful to describe low energy phenomena, and it may be correct that the virtual process of the nucleon-antinucleon pair-production plays

an important role there. However the momentum-dependence of the self-energies must be negligible below a few hundred MeV at largest, and we must treat this approach carefully when discussing phenomena above this energy.

-
- [1] B.D. Serot and J. D. Walecka, "The relativistic Nuclear Many Body Problem". In J. W. Negele and E. Vogt, editors, *Adv.Nucl.Phys.***Vol.16**, page 1, Plenum Press, 1986, and reference therein.
 - [2] B. C. Clark, S. Hama, R. L. Mercer, L. Ray and B. D. Serot, Phys. Rev. Lett. **50** (1983) 1644;
S. Hama, B. C. Clark, E. D. Cooper, H. S. Sherif and R. L. Mercer, Phys. Rev. **C41** (1990) 2737.
 - [3] J. A. Tjon and S. J. Wallace, Phys. Rev. **C36** (1987) 1085.
 - [4] W. Botermans and R. Malfliet, Phys. Rep. **198** (1990) 115;
R. Brockmann and R. Machleidt, Phys. Rev. **C42** (1990) 1965.
 - [5] D. Hirata, K. Sumiyoshi, B.V. Carlson, H. Toki, Nucl. Phys. **A609** (1996) 131.
 - [6] H. Kurasawa and T. Suzuki, Nucl. Phys. **A445** (1985) 685.
 - [7] H. Kurasawa and T. Suzuki, Nucl. Phys. **A490** (1988) 571.
 - [8] H. Kurasawa, T. Suzuki and N. Van Giai, Phys. Rev. Lett. **91** (2003) 062501.
 - [9] H. Kurasawa, T. Suzuki and N. Van Giai, Phys. Rev. **C68** (2003) 064311.
 - [10] H. Kurasawa and T. Suzuki, Phys. Rev. C **69** (2004) 014306.
 - [11] Y.S. Zhang, J.F. Liu, B.A. Robson and Y.G. Li, Phys. Rev. **C54** (1996) 332.
 - [12] S. Teis, W. Cassing, T. Maruyama and U. Mosel, Phys. Rev. **C50** (1994) 338.
 - [13] A. Schroeter et al., Nucl. Phys. **A553** (1993) 775c;
A. Schroeter et al., Z. Phys. **A350** (1994) 101.
 - [14] J. Chiba et al., Nucl. Phys. **A553** (1993) 771c;
Y. Sugaya et al., Nucl. Phys. **A634** (1998) 115.
 - [15] G.Q. Li, C.M. Ko, X.S.Fang and Y.M. Zheng, Phys. Rev. **C49** (1994) 1139.
 - [16] K. Soutome, T. Maruyama, K. Saito, Nucl. Phys. **507** (1990) 731.
 - [17] K. Weber, B. Blättel, W. Cassing, H.-C. Dönges, V. Koch, A. Lang and U. Mosel, Nucl. Phys. **A539** (1992) 713.
 - [18] C.J. Horowitz and B. D. Serot, Nucl. Phys. **A399** (1983) 529.
 - [19] T. Maruyama, B. Blättel, W. Cassing, A. Lang, U. Mosel, K. Weber, Phys. Lett **B297** (1992) 228;
T. Maruyama, W. Cassing, U. Mosel, S. Teis and K. Weber, Nucl. Phys **A552** (1994) 571.
 - [20] H. Kim, C.J. Horowitz and M.R. Frank, Phys. Rev. **C51** (1995) 792.
 - [21] T. Maruyama and S. Chiba, Phys. Rev. **C61** (2000) 037301.
 - [22] T. Maruyama and S. Chiba, Phys. Rev. **C74**, 014315 (2006).
 - [23] S. Typel, Phys. Rev. **C71** (2005) 064301.
 - [24] W. Long, H. Sagawa, J. Meng and N.V. Giai, Phys. Lett. **B639** (2006) 242.
 - [25] H. Huber, F. Weber and M. K. Weigel, Phys. Rev. **C51** (1995) 1790.
 - [26] R. Machleidt, Adv. Nucl. Phys. **19** (1989) 189.
 - [27] T. Suzuki and H. Sakai, Phys. Lett. B **455** (1999) 25.
 - [28] W. Bentz, A. Arima, H. Hyuga, K. Shimizu and K. Yazaki, Nucl. Phys. **A436** (1985) 593.
 - [29] A. Arima, W. Bentz, T. Suzuki and T. Suzuki, Phys. Lett. B **499** (2001) 104.
 - [30] G.F. Bertsch and I. Hamamoto, Phys. Rev. **C26** (1982) 1323.

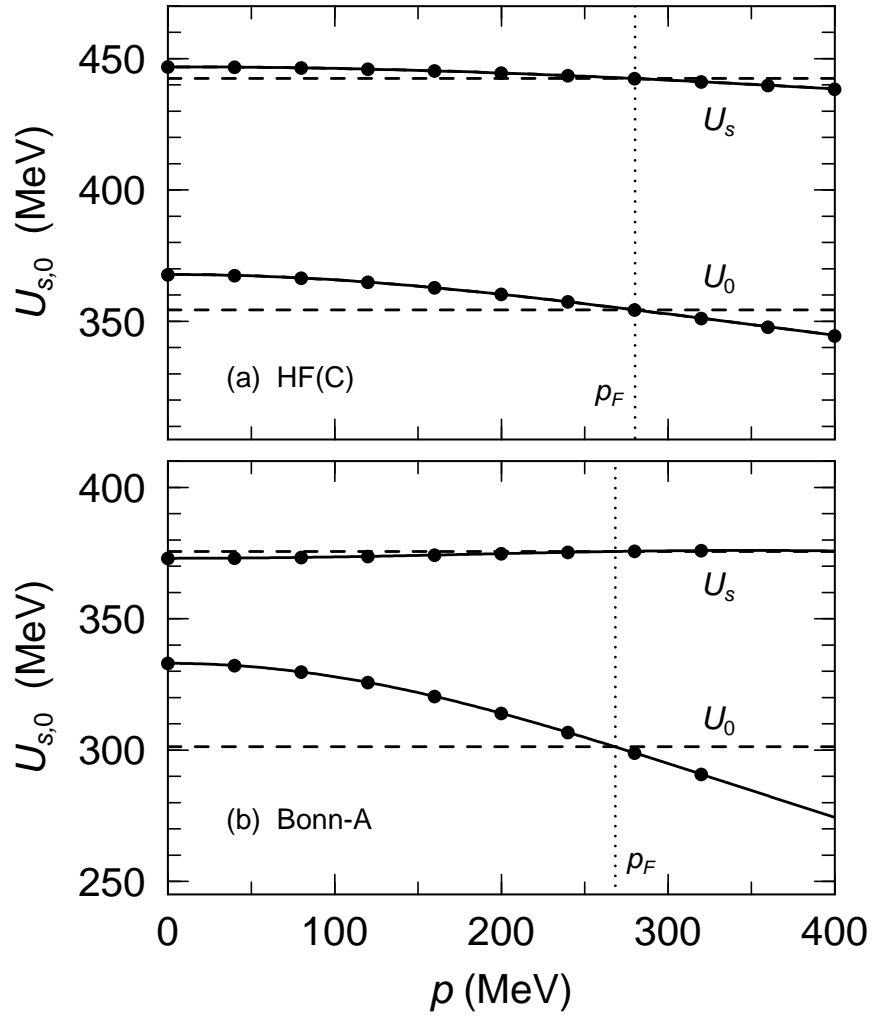


FIG. 1: Momentum-Dependence of the scalar and vector self-energies with HF(c) and Bonn-A in the upper (a) and lower panels (b). The solid and dashed lines represent the results in RHF and RH, respectively. The solid circles indicate the results of the full RHF calculation. The dotted line denotes the position of the Fermi momentum.

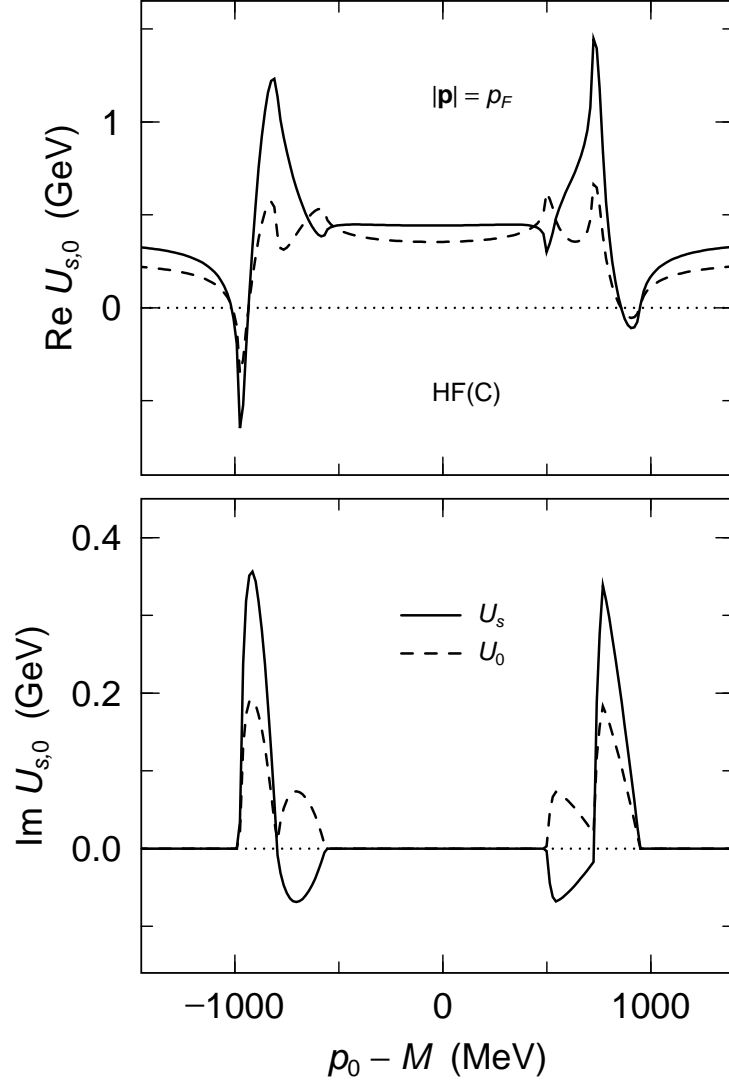


FIG. 2: The scalar and vector self-energies at $|\mathbf{p}| = k_F$ versus energy minus nucleon mass with HF(C). The solid and dashed lines represent the results of the scalar and vector self-energies, respectively.

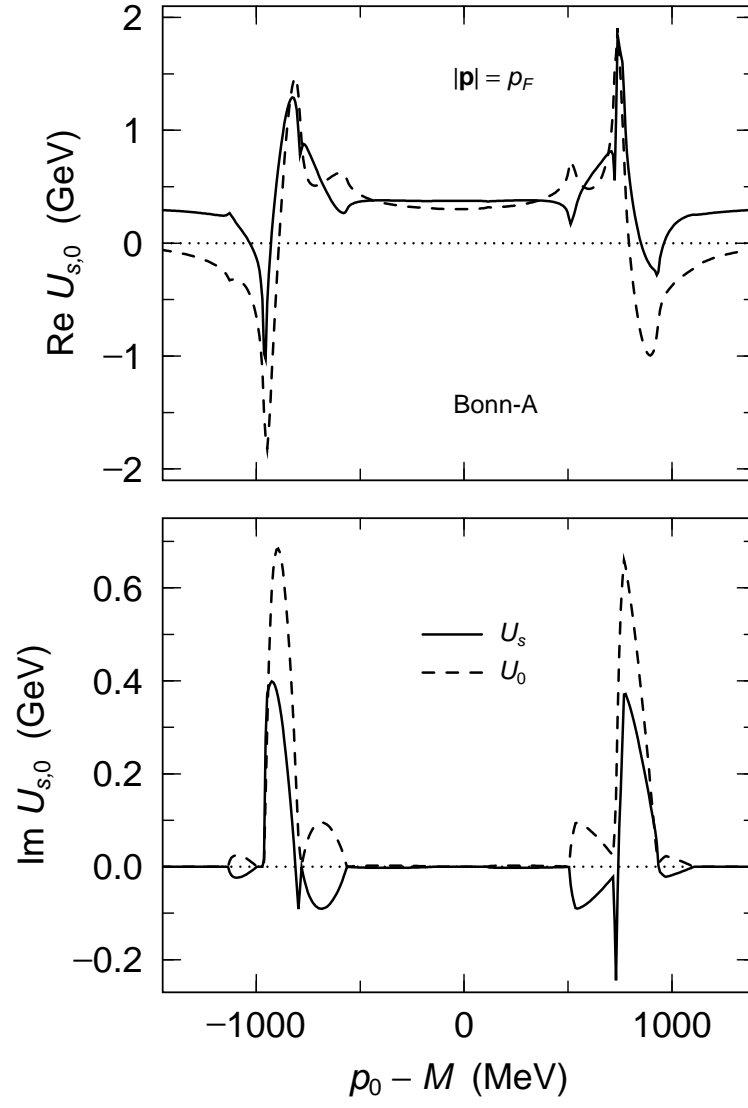


FIG. 3: The same as Fig. 2, but using the Bonn-A for the parameters.

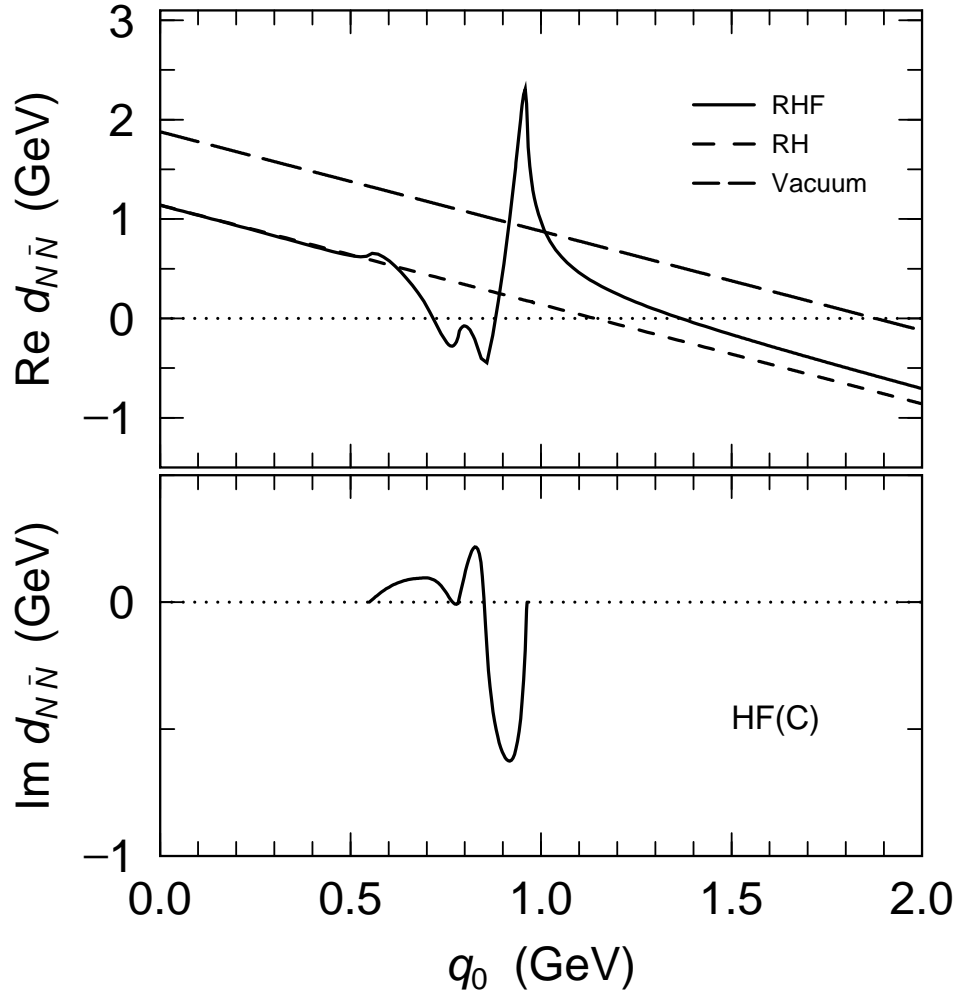


FIG. 4: The real part (a) and the imaginary part (b) of the energy denominator, $d_{N\bar{N}}$ versus the energy transfer q_0 with the parameters, HF(C). The solid and dashed lines represent the results in the RHF and RH approximations, respectively. The long-dashed line indicate the results in the vacuum.

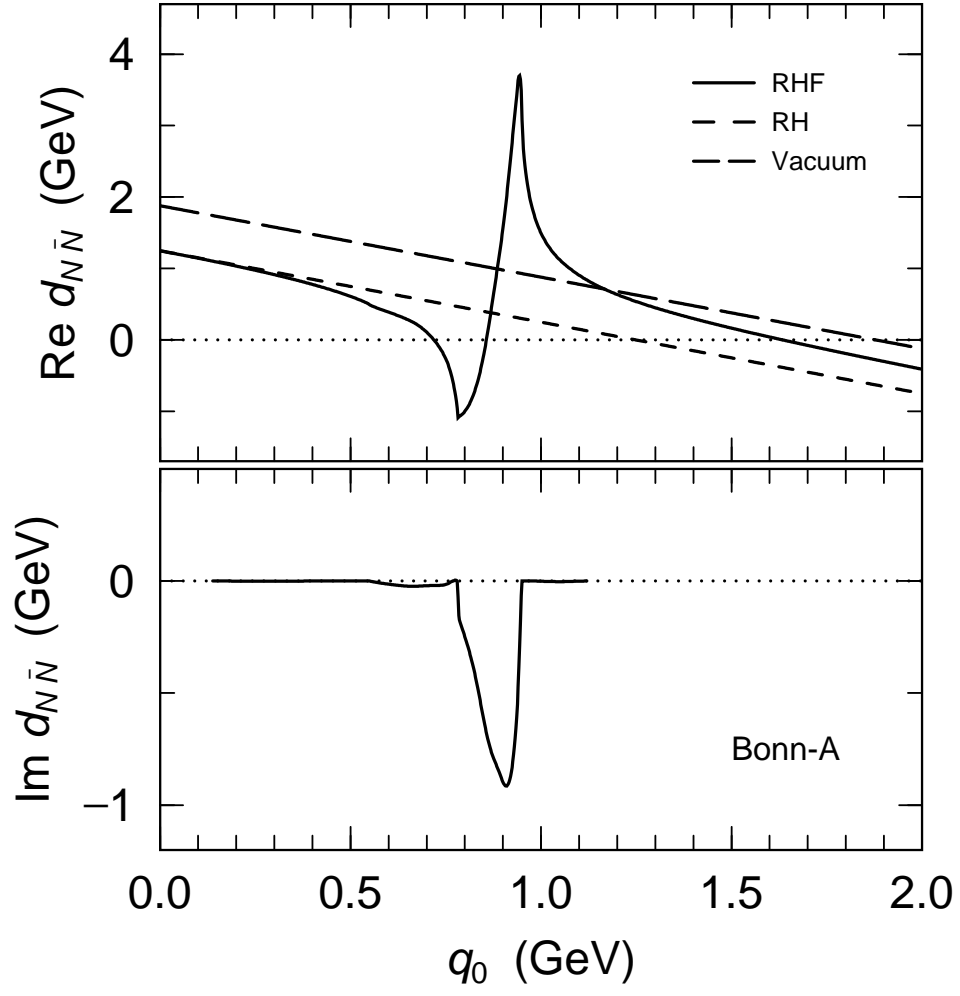


FIG. 5: The same as Fig. 4, but using the Bonn-A for the parameters.

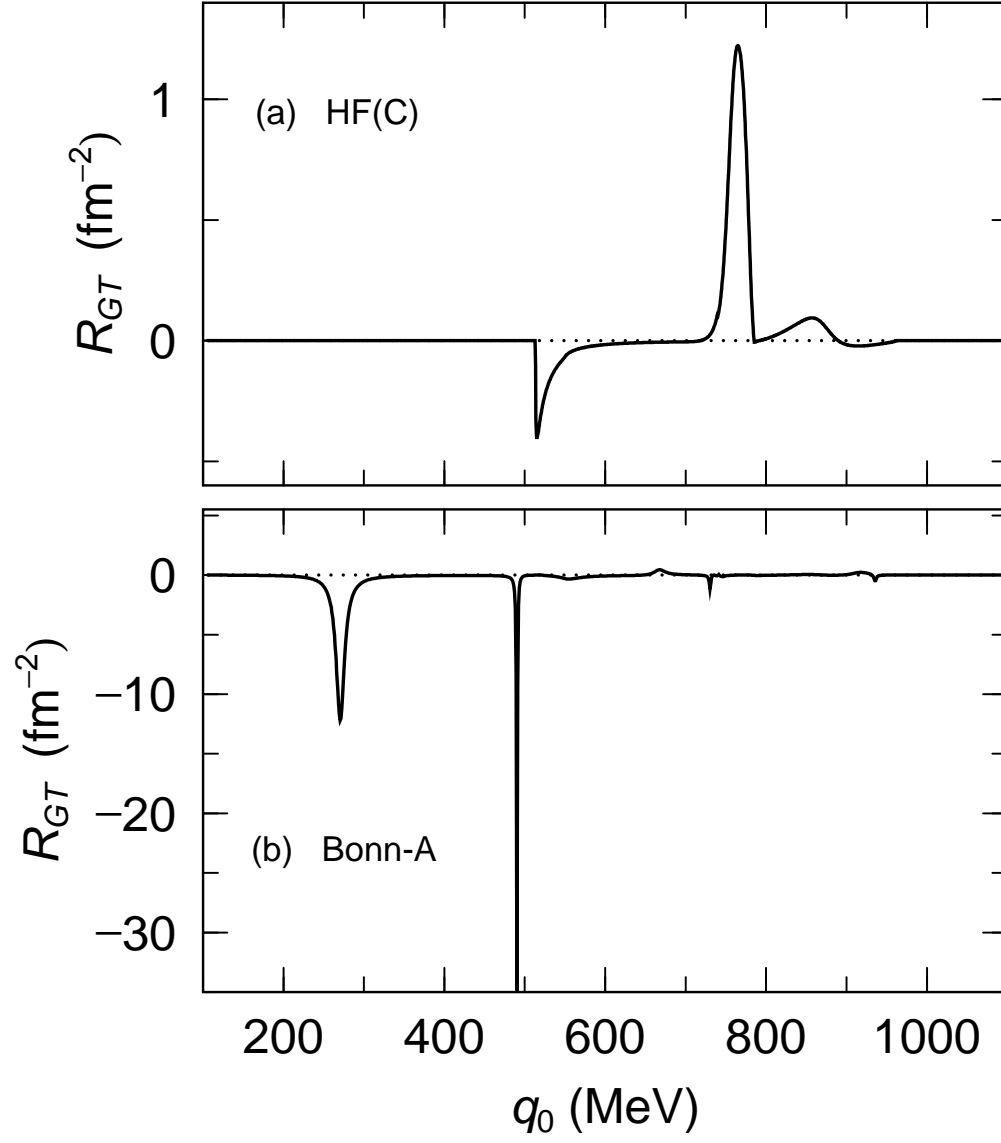


FIG. 6: The GT-response function in the meson production energy region with HF(C) (a) and Bonn-A (b).